Journal of Photochemistry and Photobiology A: Chemistry 206 (2009) 64–70

Contents lists available at ScienceDirect

Journal of Photochemistry and Photobiology A: Chemistry

journal homepage: www.elsevier.com/locate/jphotochem

Fabrication of efficient solar cells on plastic substrates using binder-free ball milled titania slurries

H.C. Weerasinghe, P.M. Sirimanne, G.P. Simon, Y.B. Cheng*

Department of Materials Engineering, Faculty of Engineering, Monash University, Welligton Road, Clayton 3800, Australia

ARTICLE INFO

Article history:
Received 6 November 2008
Received in revised form 30 March 2009
Accepted 12 May 2009
Available online 22 May 2009

Keywords:
Flexible dye sensitized solar cell
Ball milling
Electrical impedance spectroscopy

ABSTRACT

Mechanically stable, well adhered TiO_2 films based on nanocrystalline P-25 TiO_2 slurries were developed using ball milling as a part of the processing stage, without the need for binders or high temperature annealing. The strength of the TiO_2 films was examined by a novel nano-scratch technique which was developed to assess inter-particle adhesion. Interfacial and photovoltaic properties of flexible dye sensitized solar cells with a ruthenium dye involving two tetra-butyl-ammonium carboxylate groups (N719) were studied. The maximum power conversion efficiency of 4.2% is obtained under illumination of 100 mW cm^{-2}, for the electrodes fabricated using 20 h milled slurry, shorter or longer milling times were less optimal.

1. Introduction

Dye sensitized solar cells (DSSCs) have attracted much attention in research and development in recent years with the promise as a cheap alternative to the more conventional silicon solar cells. The rigidity, high cost and weight of glass substrates make the glass-based dye sensitized solar cells less likely to be mass produced and widely used. Much attention has thus recently been focused on the fabrication of light weight, flexible dye sensitized solar cells, where plastic is used as the substrate. Conventional glass-based cells are usually annealed at 450–500 °C to achieve good contact between TiO_2 particles and between the semiconductor film and conducting layer on the glass substrate. However, most polymers become unstable above ~200 °C and thus polymer-based DSSCs can only be processed at relatively low temperatures, resulting in lower conversion efficiency than the glass-based counterparts. A maximum power conversion efficiency of 6.4% has been achieved for such plastic-based dye sensitized solar cells by using an inter-particle connecting agent in the TiO_2 paste [1], compared to the maximum 11% for DSSC using glass as a substrate. Another dye sensitized cell on a plastic substrate with an efficiency of 5.8% was also reported by Durr et al. [2], but the TiO_2 films were sintered at 500 °C before being transferred to the plastic substrates by a lift-off technique for cell assembly. Therefore, finding a suitable, straightforward technique for producing plastic-based dye sensitized solar cells is one of the current key challenges in this area. Several inexpensive alternative techniques such as low temperature heating [3], microwave irradiation [4], hydrothermal crystallization [5], chemical vapour deposition [6] have all been reported as a means to deposit metal oxide films on indium tin oxide (ITO)-coated plastic substrates. The conversion efficiencies observed for these studies are close to or less than 4%. Deposition of such semiconductor films that firmly adhere to the plastic substrates is another key challenge that has to be overcome. In this work a simple technique is investigated with regards deposition of highly uniform nanocrystalline TiO_2 film on plastic substrates by using binder-free relatively cheap P-25 TiO_2 as the raw material. We have studied mechanical strength of the TiO_2 film by a new technique and investigated the photovoltaic and interfacial electrical properties of dye sensitized solar cells based on such plastic substrates.

2. Experimental

2.1. Materials

The films were made using nano-particle P-25 TiO_2 powder (Degusaa, Australia). N719 dye, *Cis*-bis (isothiocyanato) bis(2,2′-bipyridyl-4,4′-dicarboxylato)-ruthenium (II) bis-tetrabutyl-ammonium (Solaronicx SA, Switzerland) was the sensitizer. The flexible substrates used were indium tin oxide-coated polyethylene naphthalate films with a conductivity of 13 Ω cm^{-2} known as ITO|PEN (Peccell Technologies, Inc., Japan).

* Corresponding author. Tel.: +61 03 9905 4930; fax: +61 03 9905 4940.
E-mail address: Yibing.Cheng@eng.monash.edu.au (Y.B. Cheng).

1010-6030/$ – see front matter © 2009 Elsevier B.V. All rights reserved.
doi:10.1016/j.jphotochem.2009.05.013

2.2. Processing and deposition of nanocrystalline TiO_2 film on ITO/PEN substrates

Two different colloidal TiO_2 slurries were deposited on ITO|PEN substrates. Slurry A was prepared by mixing 200 mg of P-25 TiO_2 powder with 0.5 ml of ethanol in agate mortar. Surry B was prepared as follows: 7 g of P-25 TiO_2 powder and 14 ml of ethanol were placed in an agate ball milling jar with different size of agate balls. Same amount of agate balls was used through out the experiment. The mixture was then milled at 250 rpm speed for different time intervals. Both slurries were coated on the PEN substrates using either doctor blade or spin coating techniques. TiO_2 films with different thicknesses were obtained by changing the spinning speed of the spin coater or/and concentration of the slurry. TiO_2-coated ITO|PEN substrates were heated at 150 °C for 30 min, on a hotplate.

2.3. Measurements, dye absorption and fabrication of dye sensitized solar cells

The thickness and hardness of TiO_2 films were measured by a surface profilometer (Dectak 500) and by a new technique developed in this work using a nano-indenter (Hysitron Inc., USA), and further described in the text. Dye N719 was coated on TiO_2 electrodes by immersion in ethanolic dye solutions, overnight at room temperature, where the dye concentration was maintained at 0.1 mM. Dye-coated electrodes were then washed in acetonitrile and dried in flowing nitrogen.

The amount of dye absorption on TiO_2 electrodes prepared by using both ball milled and non-milled TiO_2 slurries was studied. Absorbance (or transmittance) of dye solutions and dye-coated TiO_2 electrodes was studied by a UV–vis spectrometer (Cary 5000). Dye sensitized solar cells were fabricated by attaching a Pt|ITO|PEN to the dye-coated TiO_2|ITO|PEN electrode. The electrolyte (0.04 M I_2, 0.4 M 4-tert-butylpyridine, 0.4 M lithium iodide, 0.3 M N-methylbenzimidazole in acetonitrile and 3-methoxypropionitrile by volume 1:1) was filled in between the electrodes by capillary action. Current–voltage characteristics and incident photon-to-current-conversion-efficiency of the cell with the configuration of Pt|electrolyte|N719|TiO_2 were studied under irradiation of white light (100 mWcm^{-2}) using an Oriel solar simulator system with monochromatic light. The interfacial electrical properties of the cells were studied by applying negative 0.4 V on the working electrode under a three electrode configuration, at the dark, with the same electrolyte, by using a multi-channelled potentiostat (Princeton Applied Research) coupled with a computer. The charge transfer resistance at the electrolyte–electrode interface was evaluated from EClab software.

3. Results and discussion

Fig. 1 illustrates the morphology of TiO_2 films prepared by using (a) non-milled and (b) milled slurry (20 h). As can be observed, the TiO_2 films prepared by using non-milled slurry exhibited a high level of cracking on the TiO_2 films. These cracks are essentially formed during air drying process due to the absence of binders in the TiO_2 slurry. Wider cracks are observed around agglomerates (black spots on the image Fig. 1(A)) compared to other region of the film. These wider cracks are formed due to the high stress around agglomerates on drying. However, no larger agglomerates and fewer cracks are observed on the TiO_2 films prepared by using milled slurries (Fig. 1(B)). SEM images of TiO_2 film prepared by using non-milled and milled slurries are shown as images in Fig. 1(C and D). Highly porous structures were observed for the films prepared using non-milled slurries with a more compact structure observed for films prepared following milling. De-aggregation of P-25 powder during milling is the most likely reason for the compact structure observed for the films prepared by using milled samples.

We have examined the de-aggregation of P-25 powder during ball milling by BET surface area analysis technique and the variation of the powder surface area with milling time is given in Fig. 2.

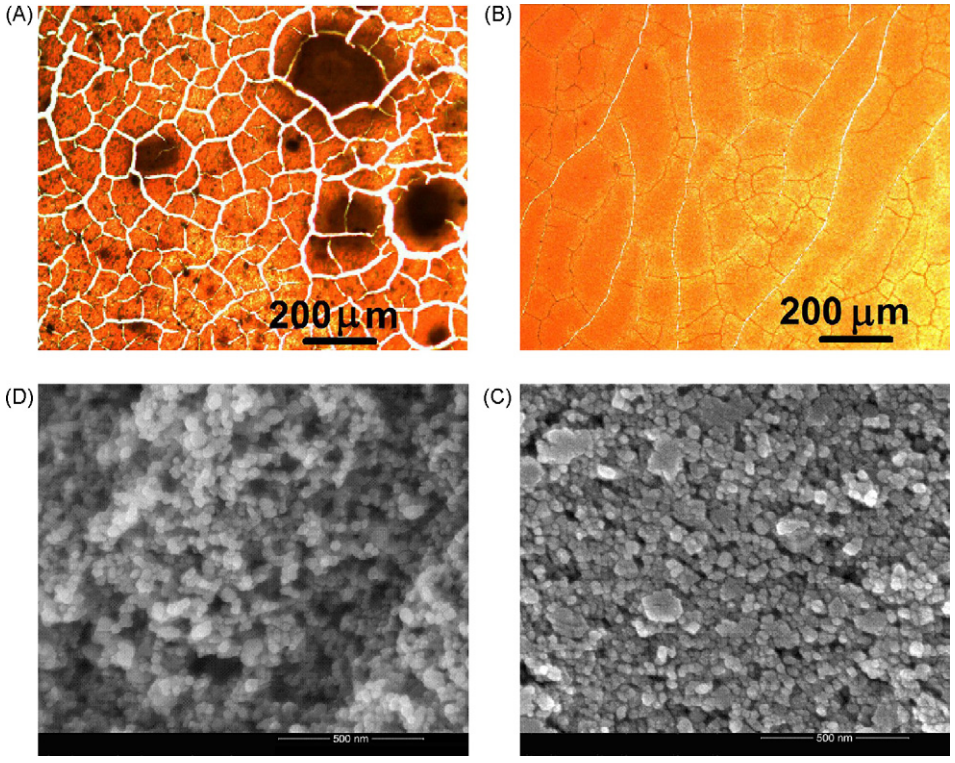

Fig. 1. Optical microscopic images of TiO_2 films prepared by using (A) non-milled and (B) milled slurries and SEM images of TiO_2 films prepared by using (C) non-milled and (D) milled samples (milled time of both samples is 20 h).

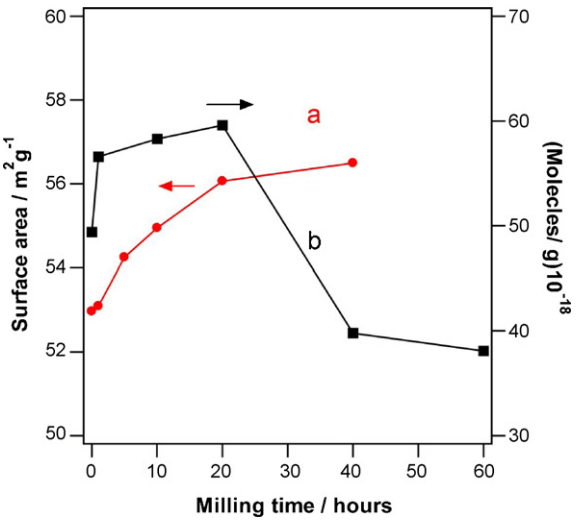

Fig. 2. The variation of (a) surface area and (b) dye absorption of TiO_2 powder with milling time.

An enhancement of surface area of TiO_2 powder was observed with increasing milling time and seems to reach a saturation level after 20 h milling. The amount of adsorbed dye on the films prepared by using TiO_2 slurries with different milling times was colorimetrically evaluated by extracting dye into ethanolic solution. The variation of dye amount on the electrode with milling time is shown as curve b in Fig. 2. The amount of dye molecules on the TiO_2 films initially increases with milling time and reaches to maxima of 60×10^{18} molecules/g after 20 h milling. An increase of dye concentration on the film is expected with increasing milling time due to the breakage of TiO_2 agglomerates. A decrease of dye amount was observed with further increasing milling time to more than 20 h. This effect was due to the contamination of the TiO_2 slurry by inclusion of silica from the agate during long term milling, which could be readily detected using an XRF spectrometer (NR XLt X-ray fluorescence analyser) (Fig. 3). We have thus chosen our experiments to be within the best observed range of milling times for TiO_2 powders, in order to achieve good photovoltaic property, namely 20–25 milling hours.

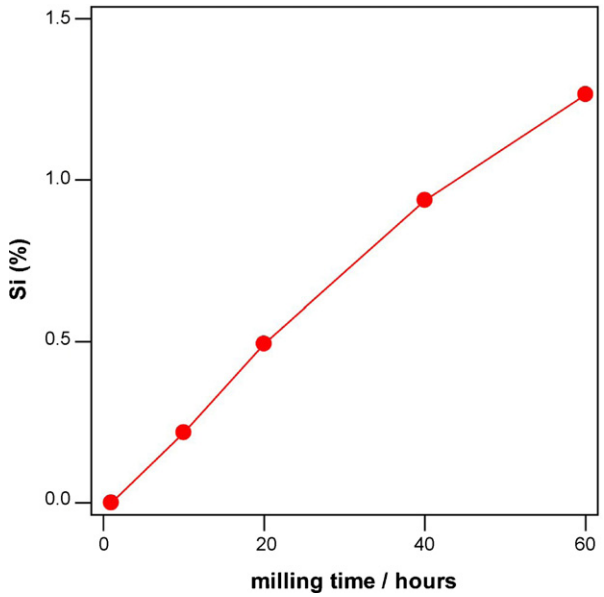

Fig. 3. Variation of Si impurity in the TiO_2 slurry with milling time, analysed using XRF.

3.1. Mechanical stability of the TiO_2 films

A good adhesion between the TiO_2 nano-particles in the porous film and between the film and the conducting substrate is essential for achieving desirable levels of electrical conductivity and thus a high efficiency of the DSSC. Mechanical strength of the porous film on the plastic substrate is a useful indication of the inter-particle connectivity in the film. The mechanical stability of the TiO_2 films prepared in this work was initially evaluated by ultra-sonication (sonicator BRANSON B550R-DTH) in an ethanol bath. An immediate and complete detachment of the TiO_2 films from plastic substrates was observed for the samples prepared using non-milled TiO_2 slurry. Stability of the film is clearly found to improve with the increase of milling time. Fig. 4 shows the variation of weight of the remaining titania film against the ultra-sonication time. To assess their mechanical integrity and adhesion, we have subjected these films to bending deformations. Films prepared using non-milled TiO_2 slurry began to detach from the substrate when bent. However, films prepared by using milled slurries (20 h and 40 h) exhibit a high degree of ongoing adhesion under bending mode compared to that of non-milled titania samples. Fig. 5 is an image of TiO_2|PEN film made with TiO_2 slurry milled for 20 h, demonstrating no peeling off during bending.

The mechanical strength of nanoporous TiO_2 films on plastic substrates has not yet been studied quantitatively, to the best of our knowledge. In this work, we are particularly interested in our ability to manipulate film quality and morphology by milling. It is thus desirable to develop a quantitative measure of the mechanical properties of the films, allowing a relative comparison of the film quality and establishing a possible correlation of the film quality and solar cell performance. The physical strength of nanoporous TiO_2 films was thus examined using a novel nano-indentation technique which measures a range of forces exerted on the indenter while performing indentation and scratch on the film. In this technique, displacement and forces in both normal and lateral directions are measured, with the probe in a displacement control mode. As can be observed, our titania films exhibit a highly porous structure (Fig. 1(C and D)). To allow for a statistic approach, a number of well spaced, and distinct scratches were made for each

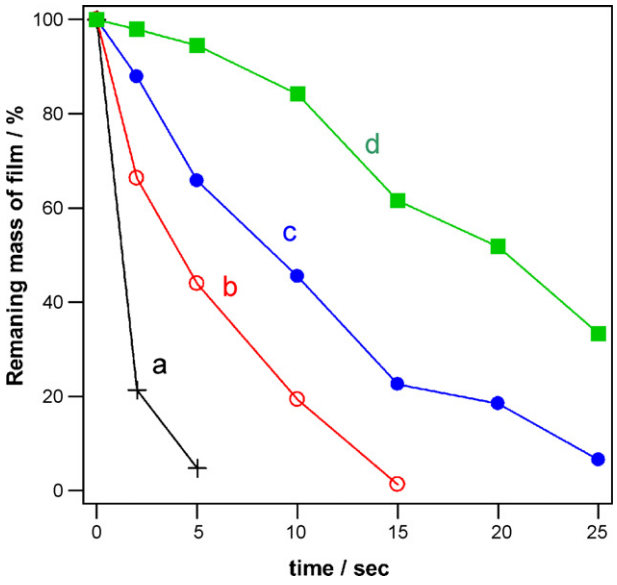

Fig. 4. Percentage of remaining mass of TiO_2 film as a function of ultra-sonication time in ethanol for films prepared using different milling times: (a) 1 h, (b) 10 h, (c) 20 h, and (d) 40 h.

Table 1
Averaged nano-indentation and nano-scratch results of maximum and steady state forces in both normal and lateral directions with increasing milling time (based on six different scratches).

Milling time (hours)	Maximum lateral force (μN)	S.D. (σ)	Maximum normal force (μN)	S.D. (σ)	Steady-state lateral force (μN)	S.D. (σ)	Steady-state normal force (μN)	S.D. (σ)
1	97	27.54	517	176.43	105	40.77	472	139.79
10	265	46.18	1636	351.89	350	33.72	1499	157.94
20	446	36.87	2748	280.60	618	45.44	2670	220.64
40	682	34.34	4310	256.07	935	29.81	4019	171.70

film with a controlled dimension of 20 μm in length and 2 μm in depth, which is much larger than the maximum pore size of the film. An average value is calculated from the multiple scratches for each sample. As the indentation depth and scratch length are fixed, the higher the normal and lateral forces recorded, the better is the inter-particle compaction in the film. Variations of normal and lateral displacements against time are shown respectively in Fig. 6(A and B). During each scratch test, the nano-indenter was initially driven into the film for a depth of 2 μm and then made a 20 μm scratch through the film following the same displacement trajectory shown in Fig. 6(A and B) and the forces excreted on the indenter during indentation and ploughing through the film were recorded. Fig. 6(C and D) illustrates a typical variation curve of the normal and lateral forces recorded with time for each sample, respectively. Significant enhancement in both the normal and lateral forces is observed with increasing milling time. The requirement of higher forces for the indentation and the scratch on films indicate the improvement of inter-particle contact in the TiO_2 film with such an increase of the milling time. Table 1 summarises the average values for the maximum normal force, lateral force (during the initial indentation) and the steady state lateral force, normal force (during the scratch) for different samples. The maximum normal force and steady state lateral force plotted against milling time are shown in Fig. 6(E and F). A similar pattern of variation was observed for both the maximum lateral force and the steady state normal force with increasing milling time as well. The linear variation of the average lateral force and maximum normal force indicates that the mechanical strength of the films has improved with increased milling time.

3.2. Impedance spectroscopy of TiO_2|dye|electrolyte cell on plastic substrate

Electrical impedance spectroscopy is a technique to examine the interfacial electrical properties of several electronic components with different kinds of junctions [7]. Fig. 7 illustrates the typical Nyquist plots for dye sensitized solar cells prepared by using TiO_2 slurry with different milling times. Two typical semicircles in Nyquist plots corresponding to high range of frequencies (1–100 kHz) and middle range of frequencies (1–1000 Hz) are observed in the order of increasing impedance. The semicircle (radius R_1) corresponding to the high range of frequencies is associated with the charge transfer at counter electrode (reduction of I_3^- at Pt electrode), and electron recombination at TiO_2|electrolyte interface together with electron transport in TiO_2 network corresponds to the semicircle with a radius of R_2 observed for middle range of frequencies [7]. The diameter of each semicircle was evaluated by using standard curve fitting software (EClab) and compared for the different samples. No significant difference is observed in values for $2R_1$ (5–7 Ω) and $2R_2$ (14–16 Ω) for the TiO_2 electrodes prepared by using non-milled and milled samples up to 40 milling hours. However, a significant enhancement in values corresponding to $2R_1$ (12 Ω) and $2R_2$ (75 Ω) is seen for the cells prepared using TiO_2 slurries exposed to long term milling (i.e. for 60 h milling). Such an enhancement of R_1 and R_2 values indicates an increase in resistance at TiO_2–TiO_2 particles, and may be attributed to the contamination of silica from agate following such long term milling. The series resistance of the cell together with connection leads (R_s) was evaluated as $15 \pm 2\ \Omega$ from the data recorded where phase is zero at the high range of frequency. Evaluated values for R_1, R_2, R_3 and R_s and plastic cells are compared with those seen in conventional glass-based DSSCs. Cells prepared using TiO_2 electrodes sintered at high temperature (i.e. at 450 °C) usually showed lower R_1, R_2, R_3 and R_s values than what we observed in this work [3], indicating the requirement of improving kinetics for charge transport at the interfaces of plastic-based DSSCs.

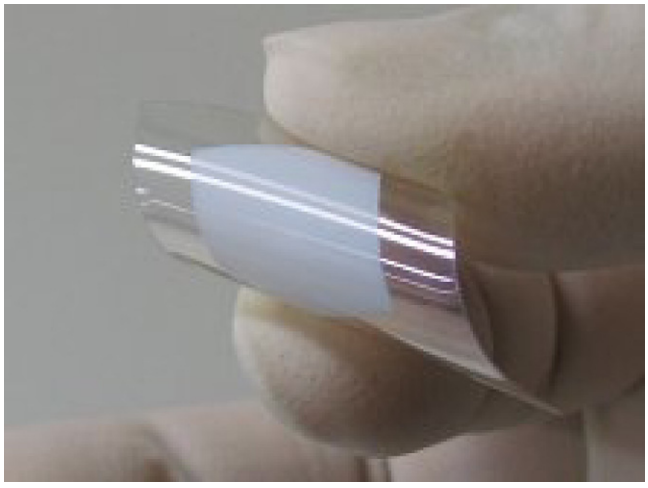

Fig. 5. Image of a bent TiO_2|PEN film made with the TiO_2 slurry milled for 20 h.

3.3. Photoelectrical properties of TiO_2|dye|electrolyte cells on plastic substrates

The incident photon-to-current efficiency (IPCE) of the cell is determined by the wavelength (λ), short circuit photocurrent (i_{ph}), and the intensity of the incident light (I_s) and is defined as the number of generated electrons divided by the number of incident photons [8] (IPCE = $1240 \times i_{ph}/(\lambda I_s)$, where, λ, I_s and i_{ph} in nm, μA cm^{-2}, μW cm^{-2}, respectively). The IPCE spectra for cells prepared by using (a) non-milled and (b) milled TiO_2 slurries are shown in Fig. 8. A maximum IPCE of 20% is observed for the cells prepared using non-milled slurries (Fig. 8a), at 525 nm, through the illumination of TiO_2 layer (back wall illumination). However, a maximum IPCE of 40% was observed for solar cells fabricated by using milled TiO_2 slurry. This value is comparable with the reported values for IPCE for fully plastic solar cells on plastic substrates prepared using hydrothermal technique by Zhang et al. [9] and the DSSC constructed by a TiO_2-coated steel electrode and a Pt-coated plastic counter electrode by Kang et al. [10]. Much higher IPCE values are achieved in conventional glass substrate-based dye sensitized solar cells where better contact is observed between the semiconductor film and conducting layer [10–14]. High temperature sintering cannot be applied dur-

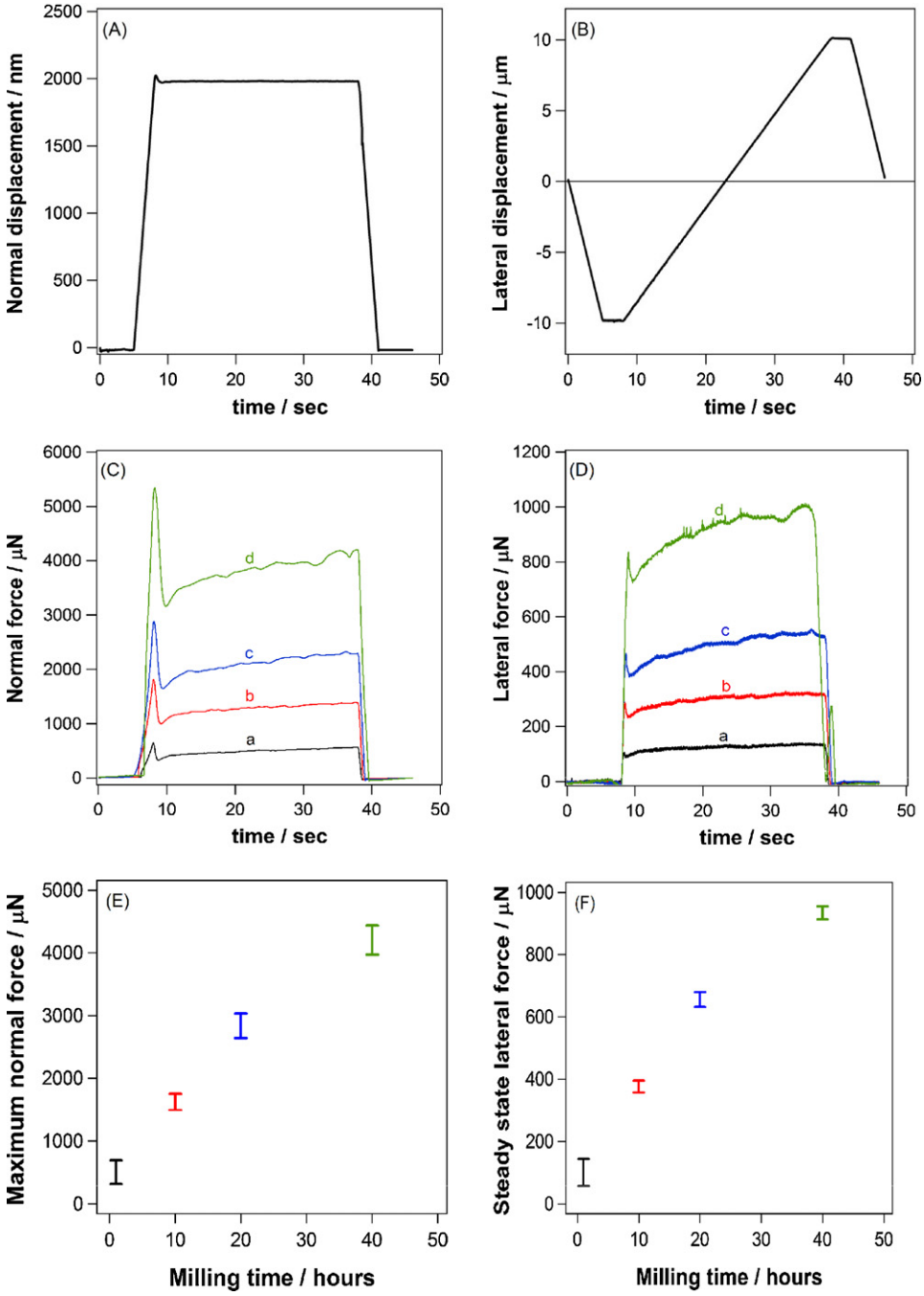

Fig. 6. The variation of (A) lateral displacement, (B) normal displacement, (C) lateral force and (D) normal force of the nano-indenter on the TiO_2 films prepared by using (a) 1 h, (b) 10 h, (c) 20 h, and (d) 40 h milled slurries. A typical measured curve was displayed for each sample. (E) Averaged maximum normal force (at $t \sim 8$ s) and (F) averaged steady state lateral force ($t \sim 35$ s) variation against milling time (the average values were calculated based on 6 different scratch tests).

ing the fabrication of plastic substrate-based solar cells due to the degradation of the substrates. As a result, weaker physical contacts exist between titania particles and the particles with the substrate, which leads to higher interfacial resistance. The hindered charge transfer process at the TiO_2 electrodes is largely responsible for the poor photovoltaic properties of the plastic substrate-based cell.

Current–voltage characteristics of the cells were also studied under white light illumination with an intensity of 100 mW cm^{-2} (Fig. 9). The cells prepared using non-milled and milled TiO_2 slurries exhibited fairly identical behaviour for the dark current conditions (curve a). A maximum short circuit photocurrent (I_{SC}) of 9.7 mA cm^{-2} and open circuit photovoltage (V_{oc}) of 635 mV are obtained for the cell prepared using the TiO_2 slurry milled for 20 h (curve c). The fill factor and conversion efficiency were 63% and 4.2% for this cell, respectively. The efficiency of the 20 h milled electrodes showed 30% increment compared to the 3.2% efficiency reported for the non-milled electrodes. These values are higher than that of the cell prepared using non-milled TiO_2 slurry (curve b) and significantly higher than those reported by Nemoto et al. (1.37%) [3] and Zhang et al. (2.5%) [9]. Our result is also highly comparable with reported values for binder-free plastic-based dye sensitized solar cells by Haque et al. [15], but is lower than the 5.6% efficiency reported by Yamaguchi et al. [16] who used an

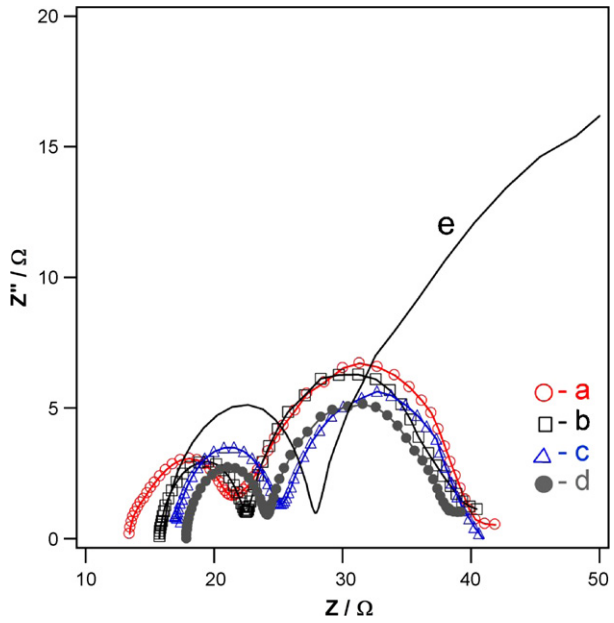

Fig. 7. Impedance spectra of Pt|electrolyte|N719|TiO_2 cells prepared by using different TiO_2 slurries with different milling times: (a) non-milled, (b) 1 h, (c) 10 h, (d) 20 h and (e) 40 h.

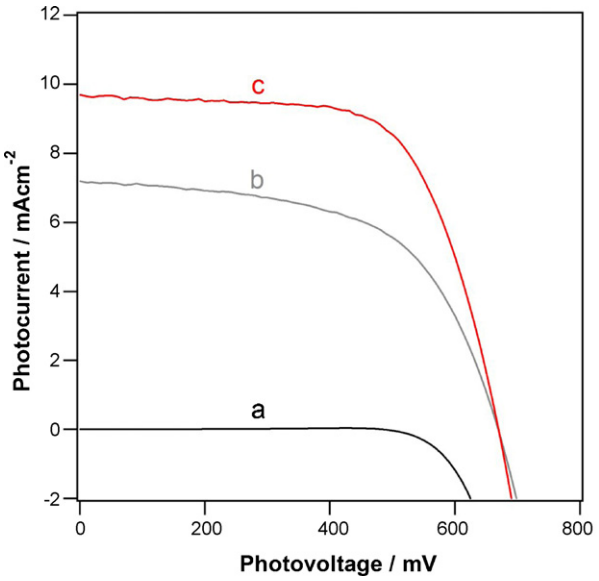

Fig. 9. Current–voltage characteristics of solar cells: (a) under the dark, and white-light conditions for the cells prepared by (b) non-milled and (c) 20 h milled TiO_2 slurries.

inter-particle connection agent. With further increase of milling time the conversion efficiency dropped down to 3.4% for the 40 h milled electrodes. This was mainly due to the decrease of dye loading of the film due to the Si contamination. The variation of photocurrent, photovoltage and efficiency with the TiO_2 film thickness in the plastic-based cells is shown in Fig. 10. The photocurrent increases significantly with increasing the film thickness until 16 μm (the maximum thickness of the film possible to avoid peeling off from the substrate in the present study). The enhancement of the photocurrent is attributed to the increase in the dye loading with the increased film thickness. The photovoltage of the cells initially increased with increasing film thickness to 0.712 V, then gradually decreased as the film thickness increased above 2.2 μm. The power conversion efficiency of the cells also varied with the film thickness, initially increasing rapidly with film thickness due to the increase of both photovoltage and current and then becoming almost unchanged due to the reduction in photocurrent for the thicker films. A similar relationship of efficiency or photocurrent variation with film thickness has been reported for the DSSCs constructed with various crystalline electrodes [17,18]. Fig. 11 illustrates the variation of maximum photocurrent with incident light intensity for the plastic-based cell prepared using 20 h milled slurry. The linear variation of the maximum photocurrent with the intensity of incident light indicates a mono-photonic process on the dye sensitized film. The efficiency of 4.2% is the highest value obtained for any plastic-based solar cell prepared using TiO_2 slurry in absence of any kind of binder or inter-particle connection agent, indicating that milling alone is an important mechanism to achieve a significant improvement in cell performance.

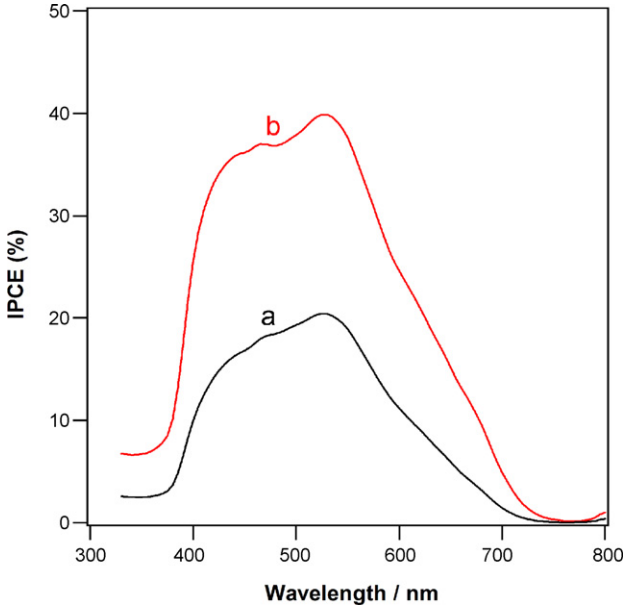

Fig. 8. IPCE spectra of Pt|electrolyte|N719|TiO_2 cells prepared by using different TiO_2 slurries: (a) non-milled and (b) milled (20 h).

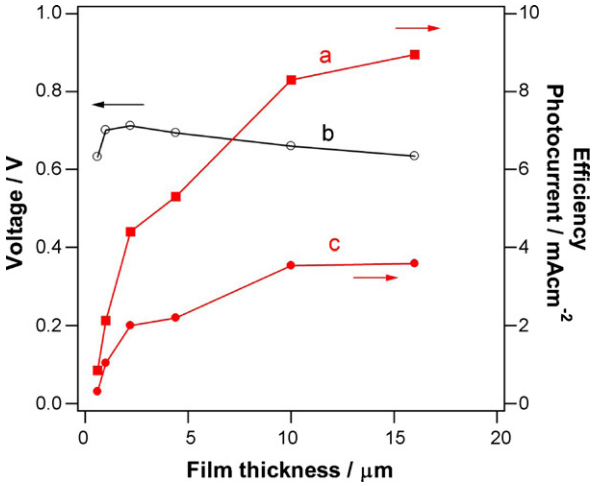

Fig. 10. The variation of (a) photocurrent, (b) photovoltage and (c) conversion efficiency with the TiO_2 film thickness of the plastic-based DSSCs.

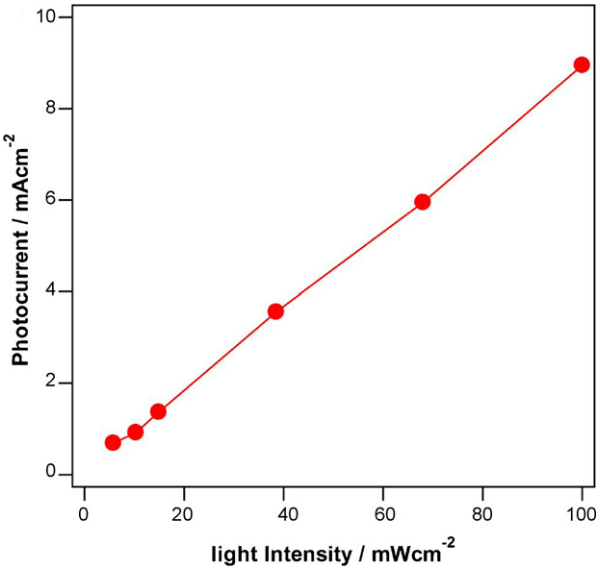

Fig. 11. The variation of the maximum photocurrent with incident light intensity for a plastic-based solar cell (TiO_2 milled for 20 h).

4. Conclusions

A simple technique was developed for the fabrication of nanoporous TiO_2 electrodes with improved mechanical stability using binder-free TiO_2 slurry. Milling of P-25 TiO_2 powder was found to increase the film quality and its mechanical stability, as well as the surface area of the titania films. A new nano-scratch technique was used to evaluate the mechanical strength of the nanoporous TiO_2 films for the first time and was found to show improved properties, in terms of strength, for the films with milling time. The improved photovoltaic performance of the DSSCs can thus be correlated with the milling time, hence the strength of the TiO_2 porous films as well as the dye loading of the films. De-agglomerization by such milling and the subsequent increase of surface area leads to higher dye adsorption on titania films and thus the maximum power conversion efficiency of 4.2% for plastic-based solar cells.

Acknowledgements

Financial supports by the Victorian Consortium in Organic Solar Cells (VICOSC) and Monash University for the scholarships are appreciated by the authors. Research facilities provided by the ARC Centre of Excellence for Electromaterials Science (ACES) and RMIT Microscopy & Microanalysis Facility (RMMF) for SEM are also appreciated.

References

[1] Y. Kijitori, M. Ikegami, T. Miyasaka, Chem. Lett. 36 (1) (2007) 190.
[2] M. Durr, A. Schmid, M. Obermaier, S. Rosselli, A. Yasuda, G. Nelles, Nat. Mater. 4 (2005) 607.
[3] J. Nemoto, M. Sakata, T. Hoshi, H. ueno, M. Kaneko, J. Electroanal. Chem. 599 (2007) 23.
[4] S. Uchida, M. Tomiha, H. Takizawa, Abstract 206 206th Meeting, The Electrochemical Society Inc., 2004.
[5] D. Zhang, T. Yoshida, H. Minoura, Adv. Mater. 15 (10) (2003) 814.
[6] T.N. Murakami, Y. Kijitori, N. Kawashima, T. Miyasaka, J. Photochem. Photobiol. A: Chem. 164 (2004) 187.
[7] D. Kuang, C. Klein, Z. Zhang, S. Ito, J.-E. Moser, S.M. Zakeeruddin, M. Gratzel, Small 3 (12) (2007) 2094.
[8] T.A. Heimer, E.J. Heilweil, C.A. Bignozzi, G.J. Meyer, J. Phys. Chem. A. 104 (2000) 4256.
[9] D. Zhang, T. Yoshida, K. Furuta, H. Minoura, J. Photochem. Photobiol. A: Chem. 164 (2004) 159.
[10] M.G. Kang, N.-G. Park, K.S. Ryu, S.H. Chang, K.-J. Kim, Solar Energy Mater. Solar Cells 90 (2006) 574.
[11] B. O'Regan, M. Gratzel, Nature 353 (1991) 737.
[12] S. Ito, T.N. Murakami, P. Comet, P. Liska, C. Gratzel, M.K. Nazeeruddin, M. Gratzel, Thin Solid Films 516 (2008) 4613.
[13] D. Kuang, P. Walter, F. Nuesch, S. Kim, J. Ko, P. Comte, S.M. Zakeeruddin, M.K. Nazeeruddin, M. Gratzel, Langmuir 23 (2007) 10906.
[14] H. Arakawa, T. Yamaguchi, A. Takeuchi, S. Agatsuma, IEEE (2006) 36.
[15] S.A. Haque, E. Palomare, H.M. Upadhyaya, L. Otley, R.J. Potter, A.B. Holmes, J.R. Durant, Chem. Commun. (2003) 3008.
[16] T. Yamaguchi, N. Tobe, D. Matsumoto, H. Arakawa, Chem. Commun. (2007) 4767.
[17] K. Tennakone, A.R. Kumarasinghe, P.M. Sirimanne, G.R.R.A. Kumara, Thin Solid Films 261 (1995) 307.
[18] K. Tennakone, A.R. Kumarasinghe, P.M. Sirimanne, Semicond. Sci. Technol. 8 (1993) 1557.